RSC Advances

PAPER

View Article Online
View Journal | View Issue

Cite this: *RSC Adv.*, 2022, **12**, 1515

Food seasoning-derived gel polymer electrolyte and pulse-plasma exfoliated graphene nanosheet electrodes for symmetrical solid-state supercapacitors†

Phuoc Anh Le, *[a] Van Qui Le,[b] Nghia Trong Nguyen [c] and Viet Bac Thi Phung *[a]

Received 22nd October 2021
Accepted 9th December 2021

DOI: 10.1039/d1ra07820h

rsc.li/rsc-advances

Kitchen sea salt or table salt is used every day by cooks as a food seasoning. Here, it is introduced into a gel polymer (poly(vinyl) alcohol (PVA)-table salt) for use as an electrolyte, and an electrode was constructed from graphene nanosheets for use as symmetrical solid-state supercapacitors. The graphene sheets are prepared by a pulse control plasma method and used as an electrode material, and were studied by X-ray diffraction (XRD), Raman spectroscopy, as well as scanning electron microscopy (SEM), transmission electron microscopy (TEM) and X-ray photoelectron spectroscopy (XPS). A specific capacitance of 117.6 F g^{-1} at 5 mV s^{-1} was obtained in a three electrode system with table sea salt as an aqueous electrolyte. For a symmetrical solid-state supercapacitor: graphene/PVA-table sea salt/graphene gave a good specific capacitance of 31.67 F g^{-1} at 0.25 A g^{-1} with an energy density of 6.33 W h kg^{-1} at a power density of 600 W kg^{-1}, with good charge–discharge stability, which was 87% after 8000 cycles. Thus, the development of table sea salt as an environmentally friendly electrolyte has a good potential for use in energy storage applications.

1 Introduction

In addition to rapidly growing demands for green resources and clean energy, it is required that the modern energy storage for the next generation of batteries, fuel cells, and supercapacitors should use high quality carbon electrode materials—in particular 2D structures—for high conductivity, good working stability, easy to make flexible electrodes, and a strong mechanical ability.[1–5]

Supercapacitors are considered to be the energy storage devices that can fill the energy gap between electrolytic capacitors and batteries with many advantages, such as fast charge–discharge, high energy density, and a long cycling life.[6–8] Typically, the symmetrical solid-state supercapacitor has a sandwich structure including one layer of a gel polymer electrolyte (GPE) between two electrode layers. In this condition, the GPEs are one of the most important keys for supercapacitor devices due to their many excellent functions. The GPE can not only be used as the protection cover for the electrode which avoids the leakage problem but also makes a strong mechanical and flexible center-layer which improves the mechanical ability and also the stability of the solid-state supercapacitor.[9–11]

During the last decade, the studies of solid-state supercapacitors based on a graphene electrode have enabled dramatic improvements in operation due to various excellent properties, such as high electrical conductivity, a strong mechanical ability, and a large surface area.[12–14] Moreover, the supercapacitors using graphene electrodes have a very low intrinsic resistance and good excellent stability.[15] Based on various types of synthesis to obtain thin layers of graphene,[16,17] cathodic plasma is one of the best ways to synthesize thin layer graphene nanosheets with high purity, and large volume in a short time.[17–19] Based on that, in this study an improved cathodic plasma method is introduced, which can be used to obtain graphene nanosheets with a higher purity.

Currently, many groups focus on GPEs for solid-state supercapacitors that use water-soluble polymers, such as PVA, PEO, and PVP as the matrix frame with a supporting acid, base, or salt as an ionic source. In the past few years, the GPE using various types of supporting inorganic and organic salts have been developed.[20–23] Although, these supporting salts have faced some serious problems with their environmentally friendliness, recycling processes, and high cost. For this reason, it is

[a]*Institute of Sustainability Science, VNU Vietnam Japan University, Vietnam National University, Hanoi 100000, Vietnam. E-mail: lephuocanh86@vnu.edu.vn; ptv.bac@vju.ac.vn*

[b]*Department of Materials Science and Engineering, National Yang Ming Chiao Tung University, Hsinchu 300093, Taiwan. E-mail: levanquidt@gmail.com*

[c]*School of Chemical Engineering, Hanoi University of Science and Technology, Hanoi 100000, Vietnam. E-mail: nghia.nguyentrong@hust.edu.vn*

† Electronic supplementary information (ESI) available. See DOI: 10.1039/d1ra07820h

necessary to find a new GPE which is environmentally friendly and at a reduced production cost. Ionic GPEs, normally use pure liquid salts which are added to gel polymers, which are considered one of the most popular GPEs. The reasons for this are that the ionic GPEs are not only cost-effective but they also have high ionic conductivity, and they can act as both ionic sources and also as a separator. In general, the acceptable cost and favorable environmentally friendliness of the ionic GPE are promising and have attracted much interest.

Herein, we report on an idea of using salt as an ionic source, which is used daily as a food seasoning: this seasoning is table salt (also called kitchen salt). For, thousands of years, table salt has been used daily as a food additive, which is made from sea water using a green production process with abundant sources, low-cost and is safe to the skin. Amazingly, table salt can dissolve completely in water to make an excellent aqueous salt electrolyte with good conductivity and thus, it makes a wonderful natural, environmentally friendly electrolyte. This paper introduces, a low-cost and safe idea of adding table salt to a gel PVA polymer to obtain a GPE PVA-table salt with a high ionic conductivity of 54 mS cm^{-1} and excellent mechanical stability. Moreover, the graphene nanosheets used are synthesized by a cathodic plasma method, which give a high quality, pure nanosheet, high electrical conductivity, and excellent stability. So far, a graphene electrode in a three electrode system using 10% aqueous table salt can reach a specific capacitance of 117.6 F g^{-1} at 5 mV s^{-1}. The symmetrical solid-state supercapacitor (graphene/PVA-table salt/graphene) had a good energy density of 6.33 W h kg^{-1} at a power density of 600 W kg^{-1}. The solid-state supercapacitor has a good retention of 87% after 8000 charge–discharge cycles. It is demonstrated that PVA-table salt will have potential prospects in energy storage device applications.

2 Experimental

2.1 Materials

Table sea salt (natural product) made in Vietnam was purchased from a local supermarket. Poly(vinylidene fluoride) (PVDF, MW: 534 000), 1-methyl-2-pyrrolidinone (NMP, C_5H_9NO) and graphite powder (<20 μm, MW: 12.01) were obtained from Sigma-Aldrich. Activated charcoal powder (MW: 12.01) was purchased from Showa. Carbon black acetylene (100% compressed) and graphite foil (10 × 10 cm, 2 mm thickness) were purchased from Alfa Aesar. Poly(vinyl alcohol) (PVA, 95% hydrolyzed, MW: 95 000) was obtained from Acros.

2.2 Preparation of exfoliated graphene nanosheets and a graphene electrode

The exfoliated graphene nanosheets used in this research were prepared by a cathodic surface-plasma exfoliation method under a regulated DC power supply (GR-15H10H, GITEK model, Taiwan). Graphite foil (1 × 3 cm) was used as a negative electrode and platinum (Pt) foil (2 × 8 cm) was used as a positive electrode. The graphite foil electrode was contacted at the surface of the electrolyte, and the Pt electrode was immersed deeply (about 6 cm) in 200 ml of aqueous electrolyte (1 M KOH) and the reaction was carried out under a voltage of 80 V at ~0.1 A for 0.5 h (Video 1, ESI†). After 30 min of cathodic surface-plasma exfoliation, the resulting mixed solution was collected and kept stable over night to obtain a black precipitate. This precipitate was collected by filtration and washed several times with 1 M HCl, deionized water and then dried overnight at 100 °C in a vacuum oven overnight to obtain the graphene material.

Graphene electrodes were prepared by a solution casting method: 8 mg of graphene (80 wt%), 1 mg of activated carbon (10 wt%) and 1 mg of PVDF (10 wt%) were dissolved in solution of NMP, with stirring over 3 d, to obtain black slurry. Then, this black slurry was coated on to a carbon paper substrate in an area of 1 × 1 cm and then dried at 80 °C for one week. Finally, one graphene electrode had a weight 1 mg cm^{-2}. For comparison, a carbon black and graphite commercial electrode were also prepared by the same steps.

The structure and morphology of the graphene nanosheets and table salt were studied by Raman spectroscopy (Horiba Jobin Yvon, using an Ar laser source with an excitation wavelength of 520 nm), XRD (Bruker D2 PHASER with a Cu Kα tube), SEM (Hitachi SU8000, using an accelerating voltage of 15 kV), TEM (Joel JEM-2100F, with an accelerating voltage of 200 kV), XPS, and auger electron spectroscopy (Microlab 350).

2.3 Preparation of aqueous and gel polymer electrolyte

The aqueous electrolyte in this study was prepared from table sea salt (10%). The salt (20 g) was added to 200 g of deionized water with constant stirring for 20 min until a clear solution was obtained. The GPE was prepared using a solution mixing method. Table salt (1 g) and 1 g of PVA were dissolved in 20 ml of deionized water with stirring at 80 °C for 3 h to obtain a homogeneous gel solution.

2.4 Electrochemical characterization

The three electrode system used a graphene or a carbon black electrode as the working electrode, Pt foil as the counter electrode and Ag/AgCl as the reference electrode and aqueous table sea salt (10%) as the electrolyte.

The symmetrical solid state supercapacitors were fabricated with a sandwich structure. The electrodes (1 × 1 cm) were immersed into gel electrolyte and allowed to dry naturally at room temperature. Then, one piece of filter paper (1 × 1 cm) was immersed deeply into the gel electrolyte and kept between two electrodes. The outside was covered with Scotch tape to make the devices (Video 2, ESI†). The electrochemical studies of the supercapacitors (cyclic voltammetry (CV), electrochemical impedance spectroscopy (EIS) and galvanostatic charge–discharge (GCD)) were carried out on an electrochemical work station (Zahner Zennium (Z 2.23), Germany).

The specific capacitance was calculated from the CV curve using the following equation:[4,5,11]

$$C = \frac{\int_{E_i}^{E_f} I(E)\mathrm{d}E}{mv(E_f - E_i)} \quad (1)$$

where E_i and E_f are the initial and final voltages of CV curves, respectively, v is the scan rate (V s^{-1}), m is the weight of the active material in the working electrode, and $(E_f - E_i)$ is the width of the potential window.

Moreover, the specific capacitance of the supercapacitor (C_i, F g^{-1}) and the symmetrical supercapacitor (SSC) device (C_s, F g^{-1}) were calculated from the charge–discharge curve, using the following equations:[4,5,11]

$$C_i = \frac{I \times \Delta t}{\Delta V \times m_{ac}} \quad (2)$$

$$C_s = 4C \quad (3)$$

The energy density (E, W h kg^{-1}) and the power density (P, W kg^{-1}) of the three electrode system and also the symmetrical devices were examined using the following equations:[4,5,11]

$$E = \frac{C_i \times (\Delta V)^2}{2} \times \frac{1000}{3600} \quad (4)$$

$$P = \frac{E \times 3600}{\Delta t} \quad (5)$$

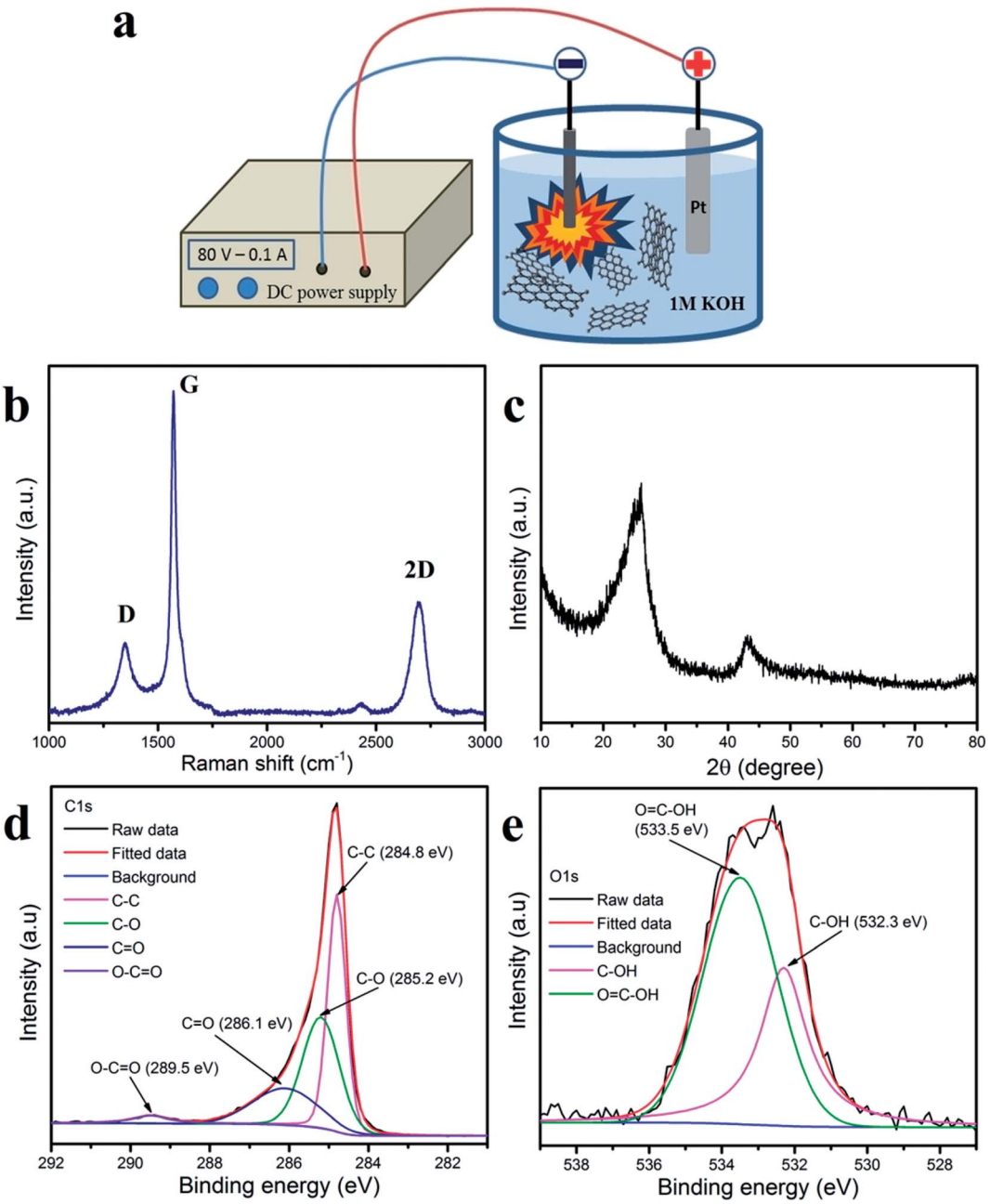

Fig. 1 (a) The cathodic plasma exfoliation process for obtaining graphene nanosheets, (b) Raman spectra, (c) XRD pattern, and XPS spectra: (d) C 1s, (e) O 1s of graphene nanosheets.

where I (A) is the discharge current, Δt is the discharge time, ΔV is the potential voltage, m_{ac} is the weight of active materials (including the binder), C_i is the capacitance of the working electrode in the three electrode system or the total capacitance in the symmetrical device system.

3 Results and discussion

3.1 Graphene nanosheets prepared by a cathodic surface-plasma exfoliation method

Herein, the graphene nanosheets were prepared using cathodic surface-plasma exfoliation and this method gave excellent quality material for use in the supercapacitor electrodes. Fig. 1a shows the cathodic plasma exfoliation process for producing graphene nanosheets in a short time at room temperature and under a low power supply. The Raman spectra of the graphene nanosheets (Fig. 1b) clearly show three peaks: D, G and 2D bands. The D band at 1350 cm^{-1} is related to the sp^2 mode of the carbon atom which corresponded to the lattice disorder, functional group bonding and defects in the structure.[24–26] The G band at about 1570 cm^{-1} originated from the phonon E_{2g} vibration mode which indicates the degree of graphitization.[27,28] Moreover, a high and symmetrical 2D band at 2696 cm^{-1}, confirmed that the presence of a few layers of graphene nanosheets left after the cathodic surface-plasma exfoliation process.[26,27] The exfoliated graphene nanosheets demonstrate a broad XRD peak at $2\theta = 26.5^\circ$ (Fig. 1c) which indicates the efficacy of the exfoliation process, which originated from the corrugation of the stacked graphene nanosheets.[29]

To determine the chemical bonding and functional groups of graphene nanosheets, the XPS spectra of C 1s and O 1s are shown in Fig. 1d and e, respectively. The deconvoluted XPS spectra of C 1s show four peaks which correspond to the functional groups of C–C (284.8 eV) of carbon sp^2, the C–O (285.2 eV) of the alkoxy group, the C=O (286.1 eV) of the carbonyl group, and the COO (289.5 eV) of the carboxyl group.[25,27,30] The O 1s spectra of the graphene nanosheets shows two peaks of C–OH (532.3 eV) and C–OOH (533.5 eV), which indicate the existence of oxygen in the carbon matrix after surface-plasma exfoliation in 1 M KOH electrolyte solution.

Fig. 2 shows the morphology of graphene nanosheets obtained using SEM and TEM. Fig. 2a and b show typical SEM images of surface-plasma exfoliated graphene nanosheets coated on a Si substrate, showing high yield graphene nanosheets with various large sizes from 2 to 10 μm. These data suggest that the surface-plasma exfoliation method can be a good strategy for preparing highly uniform graphene with a large size. Furthermore, the TEM images (Fig. 2c–e) show thin graphene sheets with random curving of the sheets which indicates that the exfoliated graphene nanosheets were comprised of a few layers which overlap with each other. A clear high-resolution TEM shows the lattice spacing of about 0.17 nm that confirms the crystalline structure and low level of defects of graphene nanosheets.[31,32] In summary, the SEM, TEM and AFM (Fig. S3, ESI†) results confirm the excellent preparation process of high quality few layered graphene nanosheets.

3.2 Environmentally friendly gel polymer electrolyte

As is demonstrated in Fig. 3, the GPE PVA-table salt was drop coated on to a glass disc and a glass tube and then dried at room temperature to form circles of dried thin film and dried thin film ribbon GPE samples. Here, the GPE (PVA-table salt) had a flexible form with a strong mechanical ability. Furthermore, Fig. 3c shows that the GPE (PVA-table salt) ribbon can be rolled

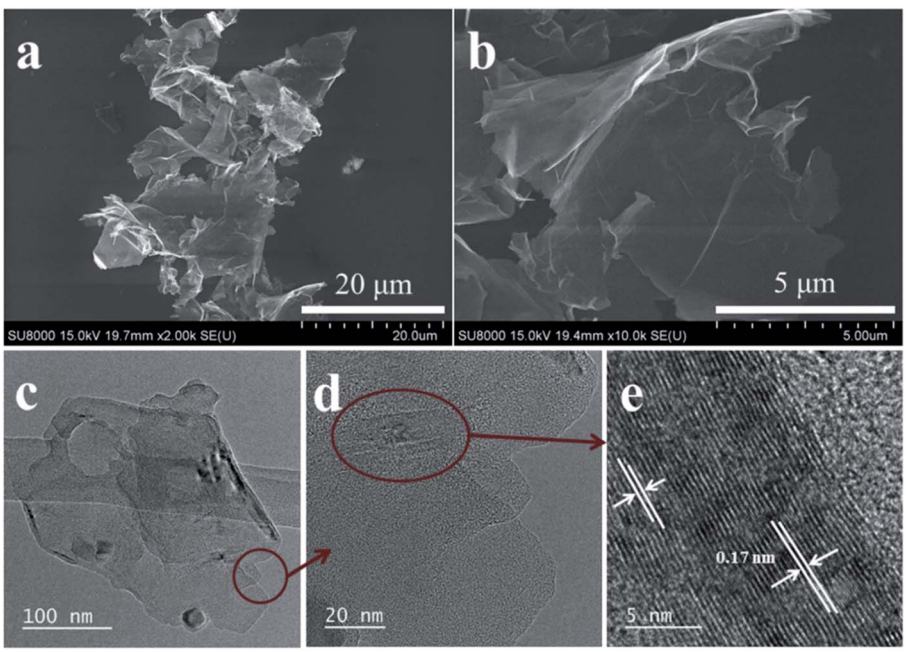

Fig. 2 (a and b) SEM images and (c–e) TEM images of graphene at various magnifications.

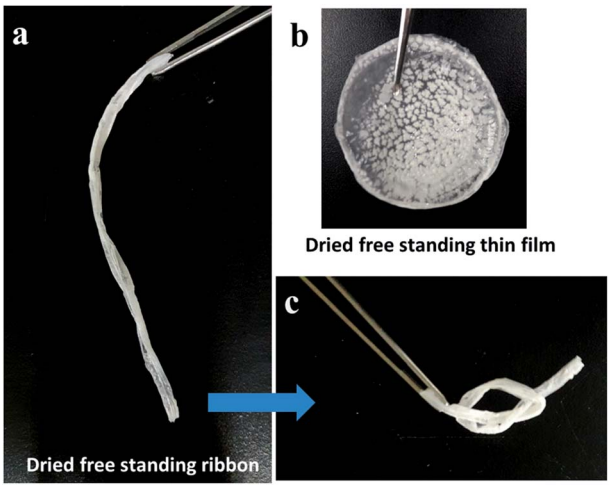

Fig. 3 (a–c) Photos were taken at room temperature of the PVA-table salt GPE.

and stretched, which indicates excellent mechanical properties. This result suggests the SSC devices have a stable electrolyte layer and also have a protected cover layer on the outside of the electrode. In this study the aqueous table sea salt (10%) gave ionic conductivity until an ionic conductivity of 128 mS cm^{-1} was reached, and the PVA-table salt GPE also reached a high ionic conductivity of 54 mS cm^{-1} which was an excellent value for the preparation of the supercapacitor electrolyte.

3.3 Electrochemical studies

3.3.1 Testing different electrode materials in the aqueous table salt electrolyte. Herein, three different electrodes: carbon black, graphite and graphene sheets in aqueous table salt electrolyte (10%) were studied. Fig. 4 shows the CV properties of three different electrodes used as the working electrode with aqueous table salt electrolyte in a three electrode system. Firstly, the CV curves of all three different working electrodes were measured from 5 to 100 mV s^{-1} with a potential window of −0.6 to 0.6 V. The CV curves showed a rectangular shape which indicated the electrochemical double layer capacitive behavior and fast ion transport behavior.[33,34] It can be seen that, the CV curves still have an increase in linearity with the increase of the scan rate which indicates the excellent stability of the working electrode in aqueous electrolyte, without any decomposition. Fig. 4d shows the specific capacitance at various scan rates following eqn (1). The graphene electrode demonstrates the highest specific capacitance when compared with graphite and carbon black. The highest capacitance of the graphene electrode was a value of 118 F g^{-1} at a scan rate of 5 mV s^{-1} which was better than that of graphite (80.3 F g^{-1}) and carbon black

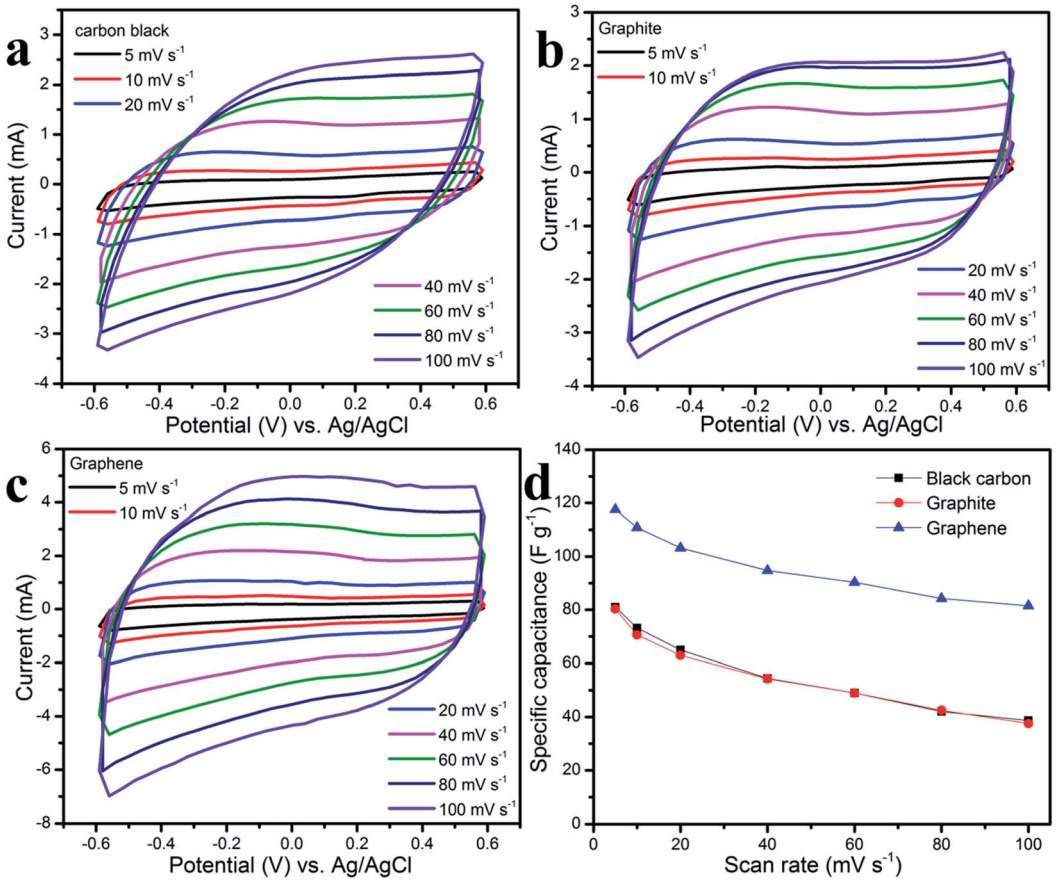

Fig. 4 The CV curves of (a) a carbon black electrode, (b) a graphite electrode, and (c) a graphene sheet electrode in aqueous table salt electrolyte. (d) The specific capacitance (F g^{-1}) at various scan rates (mV s^{-1}).

(81 F g^{-1}). Moreover, the linearity of the increasing ratio of the specific capacitance with the increase of the CV curves indicated the excellent ion diffusion at the interface of the electrode/electrolyte during the CV measurement.[35–38]

The EIS of three different working electrodes in aqueous table salt electrolyte were carried out in the frequency range from 100 mHz to 100 kHz at an amplitude of 5 mV (see Fig. 5a). In comparison, the graphene electrode has the lowest equivalent series resistance of 3.2 Ω which was lower than graphite (4.8 Ω) and carbon black (9.4 Ω). Herein, the equivalent resistance was not only the charge-transfer resistance but was also combined with the electrolyte resistance, electrode material resistance, and the resistance of the interface electrode–electrolyte.[39–41] The different equivalent series resistance values of three different working electrodes in one type of aqueous table salt electrolyte, suggest that there is a different contact resistance of the electrode–electrolyte, and a different electrode material resistance.[42,43] All the linear lines in the low frequency EIS plots indicate the capacitive effect of ion diffusion,[44] whereas the Warburg impedance arose at a high frequency as a result of the ion diffusion resistance in the electrode layer.[45] Fig. 5b–d show the charge–discharge curves with a similar triangular shape showing good capacitive behavior which was attributed to the excellent ion diffusion during the charge–

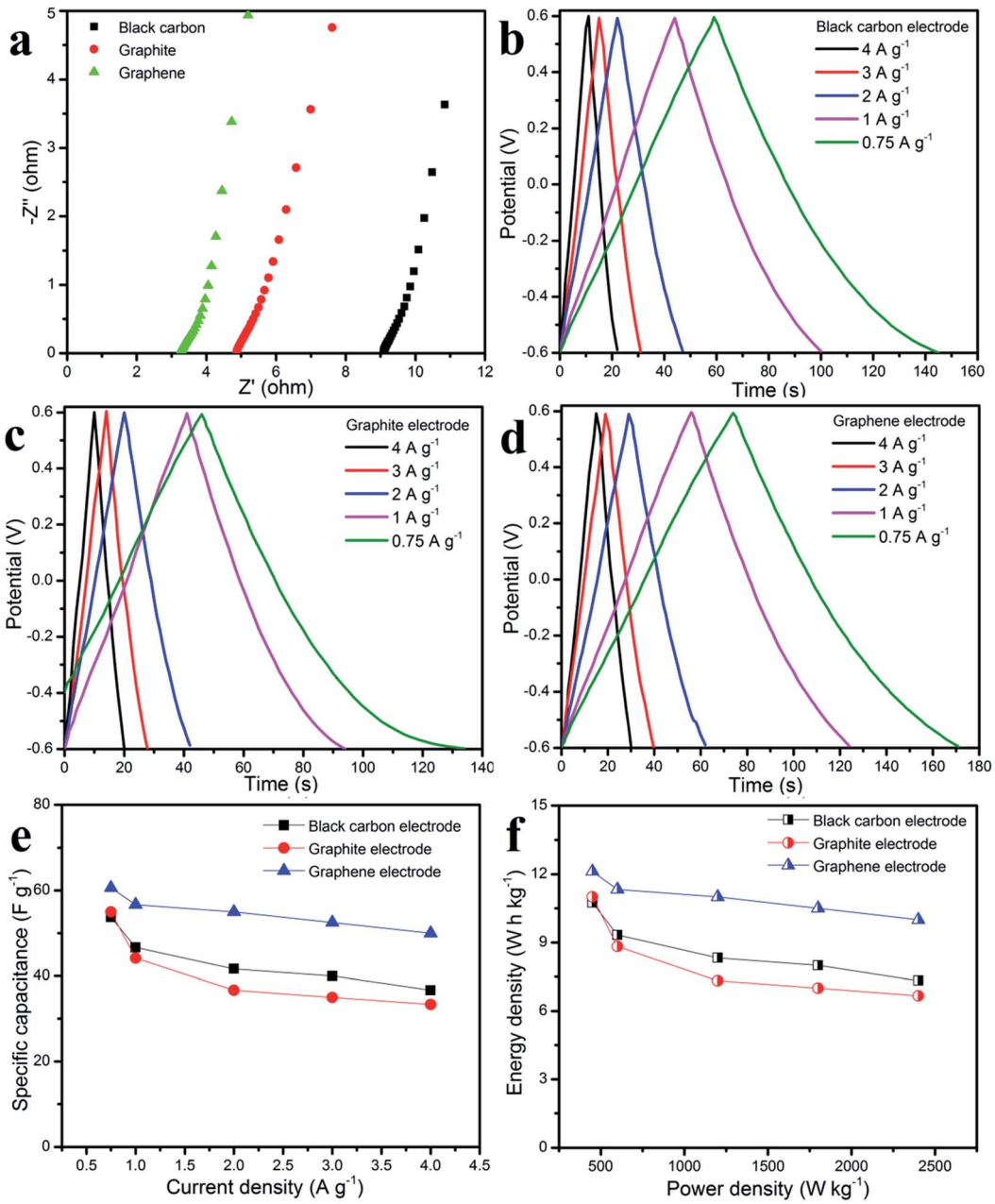

Fig. 5 The results of the electrochemical characterization performed in an aqueous table salt electrolyte: (a) EIS plots, (b–d) GCD curves, (e) specific capacitance (F g^{-1}) at various current densities (A g^{-1}), and (f) Ragone plots.

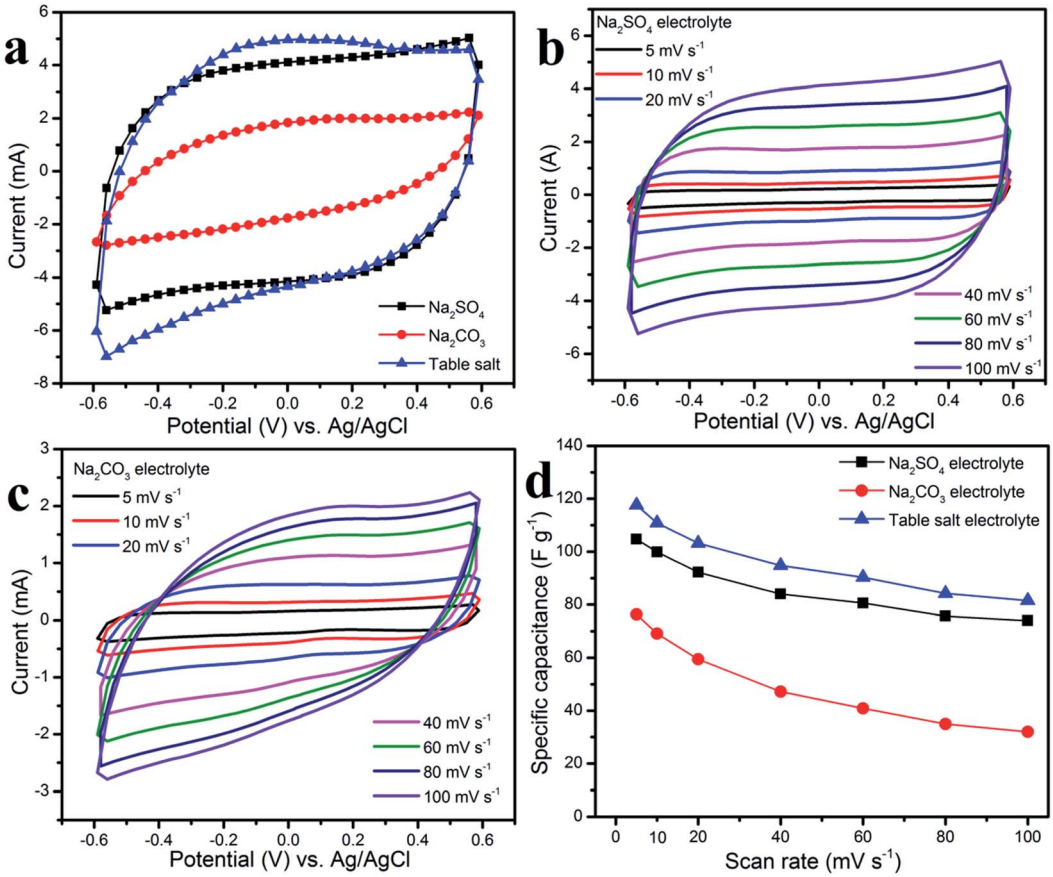

Fig. 6 (a) The CV curves of a graphene nanosheet working electrode in three different electrolytes. The CV curves at various scan rates in (b) Na_2SO_4 and (c) Na_2CO_3 aqueous electrolyte. (d) Specific capacitance (F g^{-1}) at various scan rates (mV s^{-1}).

discharge process at the interface of the electrode–electrolyte.[46,47] Following eqn (2), (4), and (5), Fig. 5e and f show the specific capacitance at various current densities, and the Ragone plots, respectively. The graphene electrode shows the highest specific capacitance of about 61 F g^{-1} which was higher than that of the graphite electrode (55 F g^{-1}) and carbon black (54 F g^{-1}) at the same current density of 0.75 A g^{-1}. At a high current density of 4 A g^{-1}, the graphene electrode still gave a good specific capacitance of 50 F g^{-1}, whereas the graphite and carbon black electrode gave values of 33.3 F g^{-1} and 36.7 F g^{-1}, respectively. From the Ragone plots, the graphene working electrode with aqueous table salt electrolyte gave the highest energy density value of 12.125 W h kg^{-1} and then the values obtained for graphite and carbon black working electrodes were: 11 W h kg^{-1} and 10.75 W h kg^{-1}, respectively, at a power density of 450 W kg^{-1}.

The results of the electrochemical studies of the three different working electrodes (graphene nanosheets, graphite, and carbon black) indicated that the electrochemical capacitive behavior was good and also that there was excellent ion diffusion at the interface of electrode–electrolyte. These results also show the high ionic conductivity and electrochemical stability of the aqueous table salt electrolyte.

3.3.2 Effect of different aqueous electrolytes on a surface-plasma exfoliation derived-graphene nanosheet electrode. For a more extensive study of the electrochemical properties of table salt as a promising candidate for a supercapacitor electrolyte, the use of three different aqueous electrolytes with a graphene working electrode was studied and compared. Fig. 6 shows the CV properties of a graphene working electrode in aqueous table salt electrolyte, compared with the same electrode 1 M Na_2CO_3 and 1 M Na_2SO_4. The electrode in table salt showed larger CV curves than the electrodes in Na_2CO_3 and Na_2SO_4 at a scan rate of 100 mV s^{-1}. All the CV curves display a quasi-rectangular shape without redox peaks, indicating the good double-layer capacitive behavior with high linearity.[48] The specific capacitances of graphene in table salt electrolyte had the highest values at various scan rates from 5 to 100 mV s^{-1}. The $C_{\text{table salt}}$ at 100 mV s^{-1} reached a value of 81.54 F g^{-1} which was higher than that of Na_2SO_4 (74 F g^{-1}) and Na_2CO_3 (32 F g^{-1}), and at 5 mV s^{-1}, the table salt had the highest specific capacitance of 118 F g^{-1} when compared with those of Na_2SO_4 (104.7 F g^{-1}) and Na_2CO_3 (76 F g^{-1}).

In addition, galvanostatic charge–discharge characterizations of the graphene working electrode in aqueous table salt electrolyte, Na_2SO_4, and Na_2CO_3 were carried out at various current densities, and the results are shown in Fig. 7a and b.

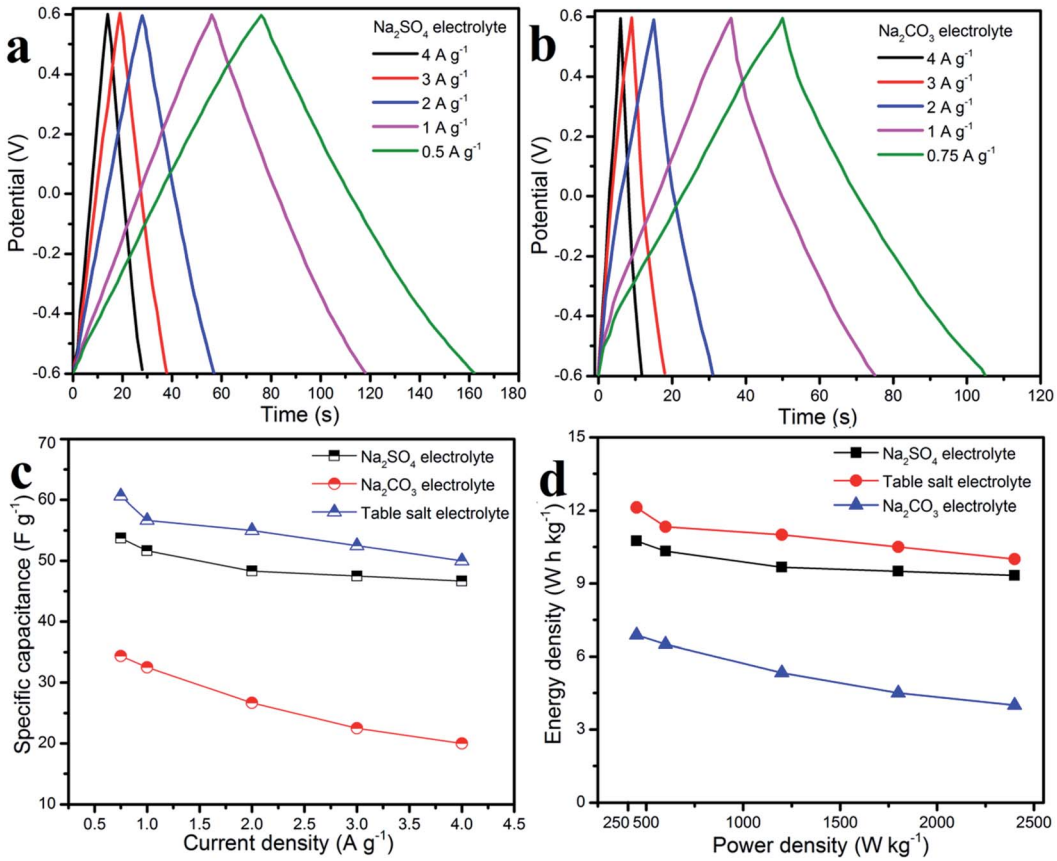

Fig. 7 The CV curves of a graphene sheet electrode in (a) Na_2SO_4 and (b) Na_2CO_3 aqueous electrolyte. (c) Specific capacitances (F g^{-1}) at various current densities (A g^{-1}). (d) Energy densities (W h kg^{-1}) at various power densities (W kg^{-1}).

The symmetrical triangular shape of the GCD curves at all scan rates indicated good electrochemical reversibility as well as a stable charge–discharge process.[49,50] The specific capacitances were calculated from the GCD curves and are shown in Fig. 7c, a high capacitance of the graphene working electrode in aqueous table salt electrolyte of up to 61 F g^{-1} at 0.75 A g^{-1} was higher than those for Na_2SO_4 and Na_2CO_3 (54 and 34 F g^{-1}, respectively). The energy density and corresponding power density shown in the Ragone plots in Fig. 7d, demonstrate a high energy density of 12 W h kg^{-1} at a power density of 450 W kg^{-1}, which far exceeded those of Na_2SO_4 (10.75 W h kg^{-1}) and Na_2CO_3 (6.9 W h kg^{-1}). Even at a high power density of 2400 W kg^{-1}, the graphene working electrode in the aqueous table salt electrolyte delivered a good energy density value of 10 W h kg^{-1} when compared with those in Na_2SO_4 (9.3 W h kg^{-1}) and Na_2CO_3 (4 W h kg^{-1}). In summary, the electrochemical properties of the graphene working electrode in an aqueous table salt electrolyte when compared with Na_2SO_4 and Na_2CO_3 confirmed the excellent chemical stability of the graphene nanosheets which were prepared by a surface-plasma exfoliation method. Moreover, these results showed that the table salt electrolyte had better ionic conductivity and ion diffusion than Na_2SO_4 and Na_2CO_3.

3.4 Symmetrical solid-state supercapacitor

Due to the outstanding electrochemical characterization of both the graphene nanosheets for working electrode and use of an aqueous table salt electrolyte, a symmetrical solid-state supercapacitor was studied which had a sandwich structure: graphene sheets/PVA-table salt/graphene sheets. The GPE was prepared by mixing PVA and table salt to obtain a homogeneous gel solution which was applied to the solid-state supercapacitors. Fig. 8 shows the electrochemical properties of the supercapacitor devices measured by CV, EIS, GCD, Ragone plots and durability. All the CV curves of the symmetrical SSCs in Fig. 8a show the nearly rectangular shape, which indicated that the supercapacitor devices had a good double layer capacitive behavior.[51] Fig. 8b shows the Nyquist plot of the supercapacitor devices over a frequency range from 100 kHz to 100 mHz at an amplitude of 5 mV. The equivalent series resistant R_s was found to be 7 Ω, which includes the intrinsic resistance of the graphene nanosheet electrode, the contact resistance of the interface electrode–electrolyte and the ionic resistance of the electrolyte.[52,53] The Nyquist plot could be divided into three parts: (i) the semicircle at high frequency related to the charge transfer resistance, (ii) a slope at about 45° in the middle frequency region related to ion diffusion from the electrolyte to the electrode layer, and (iii) the vertical line at low frequency

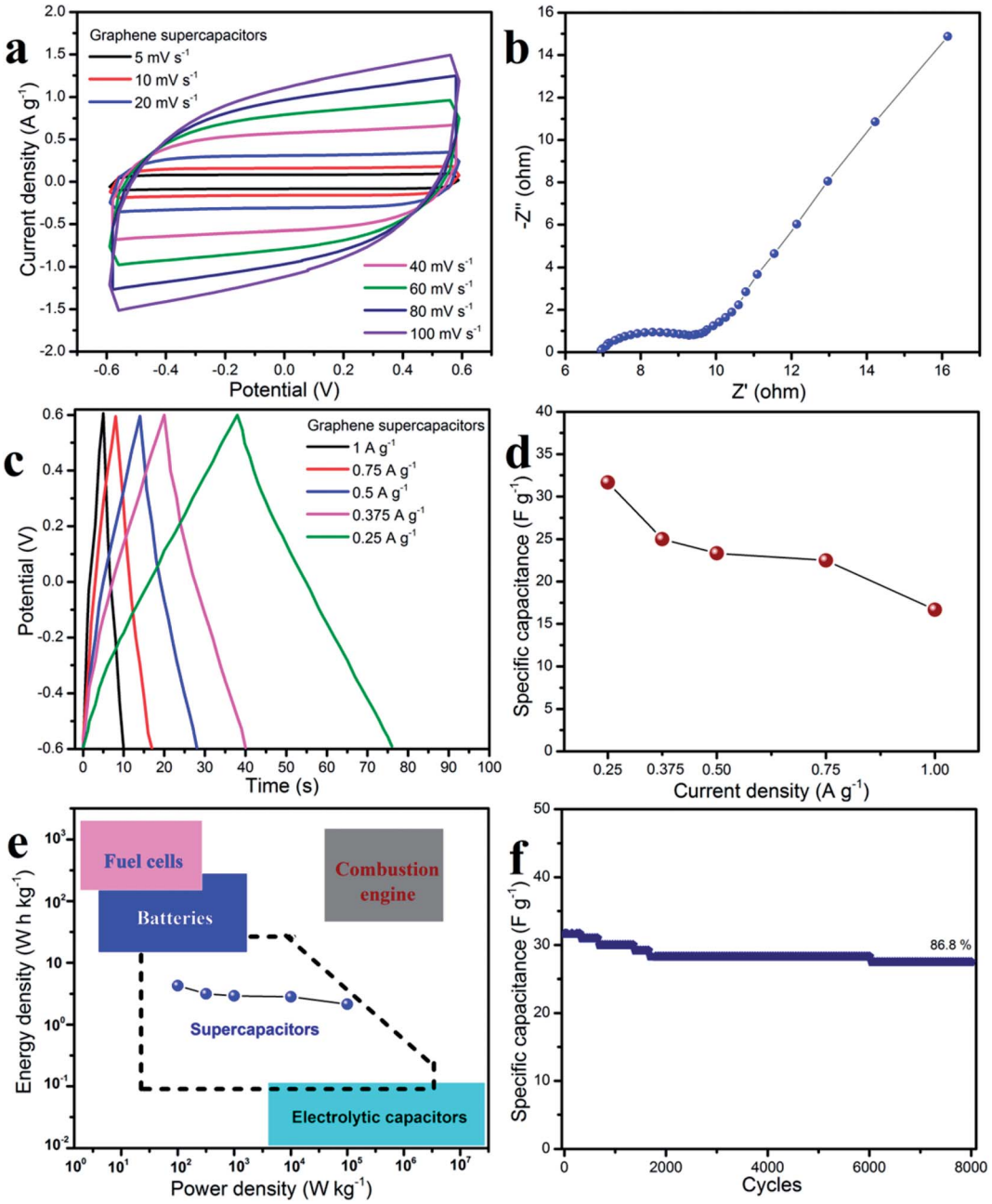

Fig. 8 Electrochemical properties of SSCs using a graphene sheet electrode: (a) CV curves, (b) EIS plot, (c) GCD curves, (d) specific capacitance as a function of current densities, (e) Ragone plot, and (f) cycling stability.

corresponding to the capacitive behavior.[54–56] Fig. 8c shows the GCD curves of the supercapacitor devices, all have symmetrical triangular shapes at various current densities (0.25–1.0 A g^{-1}) and this indicated the good electrochemical reversibility and coulombic efficiency.[57,58] The specific capacitance at various current densities could be calculated from the GCD curves based on charge–discharge time which followed eqn (3). It was clear that the symmetrical SSCs devices using PVA-table salt as a GPE exhibited a good electrochemical performance of 31.67 F g^{-1} at 0.25 A g^{-1}.

Moreover, the results of the Ragone plot satisfy the requirements for a supercapacitor (Fig. 8e) when compared with other energy storage devices. The symmetrical SSCs devices based on PVA-table salt deliver the highest energy density of 6.33 W h kg^{-1} at a power density of 600 W kg^{-1}. Even at the highest power density of 2400 W kg^{-1}, the energy density still gives a good value of 3.33 W h kg^{-1}. To investigate the durability of the symmetrical SSCs, the cycling stability was measured at a current density of 0.25 A g^{-1}. Remarkably, the supercapacitor device retained 87% of its initial value after 8000 cycles, which indicated that it would have a long-life time. These data show that PVA-table salt is a promising environmentally friendly GPE system for electrochemical supercapacitor applications.

4 Conclusions

In conclusion, an innovative, green and low-cost synthetic route was used to prepare a GPE system based on table salt as the ionic resource and graphene nanosheets as the electrode material. Graphene nanosheets, with pure and uniform quality, were prepared by a one-step of surface-plasma exfoliation method and were found to be an excellent candidate for an electrode material for supercapacitors. Moreover, a high ionic conductivity of 54 mS cm^{-1} of the GPE PVA-table salt could be applied for the fabrication of symmetrical SSCs devices which deliver a good specific capacitance of 31.67 F g^{-1} at 0.25 A g^{-1}, with strong durability after 8000 cycles (retention of 87%). This study shows a new perspective for the use of a green material, table salt as abundant green electrolyte for low-cost supercapacitors.

Author contributions

The manuscript was written with contributions from all the authors. All authors have given approval to the final version of the manuscript.

Conflicts of interest

The authors declare no competing financial interests.

Acknowledgements

This research is funded by the Vietnam National University (VNU), Hanoi (Project number: QG.20.62). The authors also wish to thank the JICA project in VNU Vietnam Japan University for providing the facilities.

References

1 K. S. Kumar, N. Choudhary, Y. Jung and J. Thomas, Recent Advances in Two-Dimensional Nanomaterials for Supercapacitor Electrode Applications, *ACS Energy Lett.*, 2018, **3**, 482–495.

2 X. Peng, L. Peng, C. Wu and Y. Xie, Two dimensional nanomaterials for flexible supercapacitors, *Chem. Soc. Rev.*, 2014, **43**, 3303–3323.

3 P. K. Panda, A. Grigoriev, Y. K. Mishra and R. Ahuja, Progress in supercapacitors: roles of two dimensional nanotubular materials, *Nanoscale Adv.*, 2020, **2**, 70–108.

4 X. Wang, A. Dong, Y. Hu, J. Qian and S. Huang, A review of recent work on using metal–organic frameworks to grow carbon nanotubes, *Chem. Commun.*, 2020, **56**, 10809–10823.

5 L. Chai, Z. Hu, X. Wang, L. Zhang, T. T. Li, Y. Hu, J. Pan, J. Qian and S. Huang, Fe_7C_3 nanoparticles with *in situ* grown CNT on nitrogen doped hollow carbon cube with greatly enhanced conductivity and ORR performance for alkaline fuel cell, *Carbon*, 2021, **15**, 531–539.

6 N. T. Nguyen, P. A. Le and V. B. T. Phung, Biomass-derived carbon hooks on Ni foam with free binder for high performance supercapacitor electrode, *Chem. Eng. Sci.*, 2021, **229**, 116053.

7 N. T. Nguyen, P. A. Le and V. B. T. Phung, Biomass-derived activated carbon electrode coupled with a redox additive electrolyte for electrical double-layer capacitors, *J. Nanopart. Res.*, 2020, **22**, 371.

8 Z. Bi, Q. Kong, Y. Cao, G. Sun, F. Su, X. Wei, X. Li, A. Ahmad, L. Xie and C. M. Chen, Biomass-derived porous carbon materials with different dimensions for supercapacitor electrodes: a review, *J. Mater. Chem. A*, 2019, **7**, 16028–16045.

9 J. Li, J. Qian and K. Lian, Hydroxide ion conducting polymer electrolytes and their applications in solid supercapacitors: A review, *Energy Storage Mater.*, 2020, **24**, 6–21.

10 Y. Guo, X. Zhou, Q. Tang, H. Bao, G. Wang and P. Saha, A self-healable and easily recyclable supramolecular hydrogel electrolyte for flexible supercapacitors, *J. Mater. Chem. A*, 2016, **4**, 8769–8776.

11 P. A. Le, V. T. Nguyen, P. J. Yen, T. Y. Tseng and K. H. Wei, A new redox phloroglucinol additive incorporated gel polymer electrolyte for flexible symmetrical solid-state supercapacitors, *Sustainable Energy Fuels*, 2019, **3**, 1536–1544.

12 M. F. E. Kady, Y. Shao and R. B. Kaner, Graphene for batteries, supercapacitors and beyond, *Nat. Rev. Mater.*, 2016, **1**, 16033.

13 Y. Shao, M. F. E. Kady, L. J. Wang, Q. Zhang, Y. Li, H. Wang, M. F. Mousavi and R. B. Kaner, Graphene-based materials for flexible supercapacitors, *Chem. Soc. Rev.*, 2015, **44**, 3639–3665.

14 J. Azadmanjiri, V. K. Srivastava, P. Kumar, M. Nikzad, J. Wang and A. Yu, Two- and three-dimensional graphene-based hybrid composites for advanced energy storage and conversion devices, *J. Mater. Chem. A*, 2018, **6**, 702–734.

15 R. K. L. Tan, S. P. Reeves, N. Hashemi, D. G. Thomas, E. Kavak, R. Montazami and N. N. Hashemi, Graphene as a flexible electrode: review of fabrication approaches, *J. Mater. Chem. A*, 2017, **5**, 17777–17803.

16 J. Liang, A. K. Mondal, D. W. Wang and F. Iacopi, Graphene-Based Planar Microsupercapacitors: Recent Advances and Future Challenges, *Adv. Mater. Technol.*, 2019, **4**, 1800200.

17 S. Y. Huang, P. A. Le, P. J. Yen, Y. C. Lu, S. K. Sahoo, H. W. Cheng, P. W. Chiu, T. Y. Tseng and K. H. Wei, Cathodic plasma induced syntheses of graphene nanosheet/MnO_2/WO_3 architectures and their use in supercapacitors, *Electrochim. Acta*, 2020, **342**, 136043.

18 V. T. Nguyen, P. A. Le, Y. C. Hsu and K. H. Wei, Plasma-Induced Exfoliation Provides Onion-Like Graphene-Surrounded MoS_2 Nanosheets for a Highly Efficient Hydrogen Evolution Reaction, *ACS Appl. Mater. Interfaces*, 2020, **12**, 11533–11542.

19 P. A. Le, V. T. Nguyen, V. Q. Le, Y. C. Lu, S. Y. Huang, S. K. Sahoo, Y. H. Chu and K. H. Wei, One-Step Surface-Plasma-Induced Exfoliation of the Graphite/WS_2 Bilayer into Homogeneous Two-Dimensional Graphene/WS_2 Nanosheet Composites as Catalysts for the Hydrogen Evolution Reaction, *ACS Appl. Energy Mater.*, 2021, **4**, 5143–5154.

20 L. Xia, L. Yu, D. Hu and G. Z. Chen, Electrolytes for electrochemical energy storage, *Mater. Chem. Front.*, 2017, **1**, 584–618.
21 X. Zhang, L. L. Wang, J. Peng, P. F. Cao, X. S. Cai, J. Q. Li and M. L. Zhai, A Flexible Ionic Liquid Gelled PVA-Li_2SO_4 Polymer Electrolyte for Semi-Solid-State Supercapacitors, *Adv. Mater. Interfaces*, 2015, 1500267.
22 F. Yu, M. L. Huang, J. Wu, Z. Y. Qiu, L. Q. Fan, J. M. Lin and Y. B. Lin, A Redox-Mediator-Doped Gel Polymer Electrolyte Applied in Quasi-Solid-State Supercapacitors, *J. Appl. Polym. Sci.*, 2014, **131**, 39784.
23 H. Wang, J. Chen, R. Fan and Y. Wang, A flexible dual solid-state electrolyte supercapacitor with suppressed self-discharge and enhanced stability, *Sustainable Energy Fuels*, 2018, **2**, 2727–2732.
24 F. Ouhib, A. Aqil, J. M. Thomassin, C. Malherbe, B. Gilbert, T. S. Lanero, A. S. Duwez, F. Deschamps, N. Job, A. Vlad, S. Melinte, C. Jérôme and C. Detrembleur, A facile and fast electrochemical route to produce functional few-layer graphene sheets for lithium battery anode application, *J. Mater. Chem. A*, 2014, **2**, 15298–15302.
25 C. H. Chen, S. W. Yang, M. C. Chuang, W. Y. Woon and C. Y. Su, Towards the continuous production of high crystallinity graphene *via* electrochemical exfoliation with molecular *in situ* encapsulation, *Nanoscale*, 2015, **7**, 15362–15373.
26 N. Parveen, M. O. Ansari and M. H. Cho, Simple route for gram synthesis of less defective few layered graphene and its electrochemical performance, *RSC Adv.*, 2015, **5**, 44920–44927.
27 S. Tian, P. He, L. Chen, H. Wang, G. Ding and X. Xie, Electrochemical Fabrication of High Quality Graphene in Mixed Electrolyte for Ultrafast Electrothermal Heater, *Chem. Mater.*, 2017, **29**, 6214–6219.
28 C. N. R. Rao, A. K. Sood, K. S. Subrahmanyam and A. Govindaraj, Graphene: The New Two-Dimensional Nanomaterial, *Angew. Chem., Int. Ed.*, 2009, **48**, 7752–7777.
29 K. Chen, D. Xue and S. Komarneni, Nanoclay assisted electrochemical exfoliation of pencil core to high conductive graphene thin-film electrode, *J. Colloid Interface Sci.*, 2017, **487**, 156–161.
30 L. Lu, C. Zeng, L. Wang, X. Yin, S. Jin, A. Lu and Z. J. Ren, Graphene oxide and H_2 production from bioelectrochemical graphite oxidation, *Sci. Rep.*, 2015, **5**, 16242.
31 C. H. Chuang, C. Y. Su, K. T. Hsu, C. H. Chen, C. H. Huang, C. W. Chu and W. R. Liu, A green, simple and cost-effective approach to synthesize high quality graphene by electrochemical exfoliation *via* process optimization, *RSC Adv.*, 2015, **5**, 54762–54768.
32 A. R. Kamali and D. J. Fray, Large-scale preparation of graphene by high temperature insertion of hydrogen into graphite, *Nanoscale*, 2015, **7**, 11310–11320.
33 L. Cao, M. Yang, D. Wu, F. Lyu, Z. Sun, X. Zhong, H. Pan, H. Liu and Z. Lu, Biopolymer-chitosan based supramolecular hydrogels as solid state electrolytes for electrochemical energy storage, *Chem. Commun.*, 2017, **53**, 1615–1618.
34 Z. Song, H. Duan, D. Zhu, Y. Lv, W. Xiong, T. Cao, L. Li, M. Liu and L. Gan, Ternary-doped carbon electrodes for advanced aqueous solid-state supercapacitors based on a "water-in-salt" gel electrolyte, *J. Mater. Chem. A*, 2019, **7**, 15801–15811.
35 J. Piwek, A. Platek, K. Fic and E. Frackowiak, Carbon-based electrochemical capacitors with acetate aqueous electrolytes, *Electrochim. Acta*, 2016, **215**, 179–186.
36 C. Zequine, C. K. Ranaweera, Z. Wang, S. Singh, P. Tripathi, O. N. Srivastava, B. K. Gupta, K. Ramasamy, P. K. Kahol, P. R. Dvornic and R. K. Gupta, High Performance and Flexible Supercapacitors based on Carbonized Bamboo Fibers for Wide Temperature Applications, *Sci. Rep.*, 2017, **6**, 31704.
37 S. Bhoyate, C. K. Ranaweera, C. Zhang, T. Morey, M. Hyatt, P. K. Kahol, M. Ghimire, S. R. Mishra and R. K. Gupta, Eco-Friendly and High Performance Supercapacitors for Elevated Temperature Applications Using Recycled Tea Leaves, *Global Challenges*, 2017, **1**, 1700063.
38 P. Sirisinudomkit, P. Iamprasertkun, A. Krittayavathananon, T. Pettong, P. Dittanet and M. Sawangphruk, Hybrid Energy Storage of $Ni(OH)_2$-coated N-doped Graphene Aerogel//N-doped Graphene Aerogel for the Replacement of NiCd and NiMH Batteries, *Sci. Rep.*, 2017, **7**, 1124.
39 M. S. Javed, C. Zhang, L. Chen, Y. Xi and C. Hu, Hierarchical mesoporous $NiFe_2O_4$ nanocone forest directly growing on carbon textile for high performance flexible supercapacitors, *J. Mater. Chem. A*, 2016, **4**, 8851–8859.
40 C. Chi, Y. Li, D. Li, H. Huang, Q. Wang, Y. Yang and B. Huang, Flexible solvent-free supercapacitors with high energy density enabled by electrical-ionic hybrid polymer nanocomposites, *J. Mater. Chem. A*, 2019, **7**, 16748–16760.
41 X. Sun, H. Lu, T. E. Rufford, R. R. Gaddam, T. T. Duignan, X. Fan and X. S. Zhao, A flexible graphene – carbon fiber composite electrode with high surface area-normalized capacitance, *Sustainable Energy Fuels*, 2019, **3**, 1827–1832.
42 Y. Guo, X. Zhou, Q. Tang, H. Bao, G. Wang and P. Saha, A self-healable and easily recyclable supramolecular hydrogel electrolyte for flexible supercapacitors, *J. Mater. Chem. A*, 2016, **4**, 8769–8776.
43 J. Wang, B. Ding, Y. Xu, L. Shen, H. Dou and X. Zhang, Crumpled Nitrogen-Doped Graphene for Supercapacitors with High Gravimetric and Volumetric Performances, *ACS Appl. Mater. Interfaces*, 2015, **7**, 22284–22291.
44 Y. K. Ahn, B. Kim, J. Ko, D. J. You, Z. Yin, H. Kim, D. Shin, S. Cho, J. Yoo and Y. S. Kim, All solid state flexible supercapacitors operating at 4 V with a cross-linked polymer – ionic liquid electrolyte, *J. Mater. Chem. A*, 2016, **4**, 4386–4391.
45 D. Liu, Q. Li and H. Zhao, Electrolyte-assisted hydrothermal synthesis of holey graphene films for all-solid-state supercapacitors, *J. Mater. Chem. A*, 2018, **6**, 11471–11478.
46 C. Yin, X. Liu, J. Wei, R. Tan, J. Zhou, M. Ouyang, H. Wang, S. J. Cooper, B. Wu, C. George and Q. Wang, "All-in-Gel" design for supercapacitors towards solid-state energy

devices with thermal and mechanical compliance, *J. Mater. Chem. A*, 2019, **7**, 8826–8831.

47 D. Li, Z. Xu, X. Ji, L. Liu, G. Gai, J. Yang and J. Wang, Deep insight into ionic transport in polyampholyte gel electrolytes towards high performance solid supercapacitors, *J. Mater. Chem. A*, 2019, **7**, 16414–16424.

48 N. R. Raap, M. Enterría, J. I. Martins, M. F. R. Pereira and J. L. Figueiredo, Influence of Multiwalled Carbon Nanotubes as Additives in Biomass-Derived Carbons for Supercapacitor Applications, *ACS Appl. Mater. Interfaces*, 2019, **11**, 6066–6077.

49 L. Yang, B. Gu, Z. Chen, Y. Yue, W. Wang, H. Zhang, X. Liu, S. Ren, W. Yang and Y. Li, Synthetic Biopigment Supercapacitors, *ACS Appl. Mater. Interfaces*, 2019, **11**, 30360–30367.

50 C. L. Ban, Z. Xu, D. Wang, Z. Liu and H. Zhang, Porous Layered Carbon with Interconnected Pore Structure Derived from Reed Membranes for Supercapacitors, *ACS Sustainable Chem. Eng.*, 2019, **7**, 10742–10750.

51 L. Yu, L. Hu, B. Anasori, Y. T. Liu, Q. Zhu, P. Zhang, Y. Gogotsi and B. Xu, MXene-Bonded Activated Carbon as a Flexible Electrode for High-Performance Supercapacitors, *ACS Energy Lett.*, 2018, **3**, 1597–1603.

52 K. Ghosh, C. Y. Yue, M. M. Sk, R. K. Jena and S. Bi, Development of a 3D graphene aerogel and 3D porous graphene/MnO_2@polyaniline hybrid film for all-solid-state flexible asymmetric supercapacitors, *Sustainable Energy Fuels*, 2018, **2**, 280–293.

53 D. Jiang, J. Zhang, C. Li, W. Yang and J. Liu, A simple and large-scale method to prepare flexible hollow graphene fibers for a high-performance all-solid fiber supercapacitor, *New J. Chem.*, 2017, **41**, 11792–11799.

54 A. K. Nayak, A. K. Das and D. Pradhan, High Performance Solid-State Asymmetric Supercapacitor using Green Synthesized Graphene–WO_3 Nanowires Nanocomposite, *ACS Sustainable Chem. Eng.*, 2017, **5**(11), 10128–10138.

55 H. Fan and W. Shen, Gelatin-Based Microporous Carbon Nanosheets as High Performance Supercapacitor Electrodes, *ACS Sustainable Chem. Eng.*, 2016, **4**, 1328–1337.

56 L. Hu, Q. Zhu, Q. Wu, D. Li, Z. An and B. Xu, Natural Biomass-Derived Hierarchical Porous Carbon Synthesized by an *in Situ* Hard Template Coupled with NaOH Activation for Ultrahigh Rate Supercapacitors, *ACS Sustainable Chem. Eng.*, 2018, **6**, 13949–13959.

57 X. Wang, S. Yun, W. Fang, C. Zhang, X. Liang, Z. Lei and Z. Liu, Layer-Stacking Activated Carbon Derived from Sun flower Stalk as Electrode Materials for High-Performance Supercapacitors, *ACS Sustainable Chem. Eng.*, 2018, **6**, 11397–11407.

58 B. Krüner, A. Schreiber, A. Tolosa, A. Quade, F. Badaczewski, T. Pfaff, B. M. Smarsly and V. Presser, Nitrogen-containing novolac-derived carbon beads as electrode material for supercapacitors, *Carbon*, 2018, **132**, 220–231.